

Modular Chemistry: Secondary Building Units as a Basis for the Design of Highly Porous and Robust Metal–Organic Carboxylate Frameworks

MOHAMED EDDAOUDI,[†] DAVID B. MOLER,[†]
HAILIAN LI,[†] BANGLIN CHEN,[†]
THERESA M. REINEKE,[‡]
MICHAEL O'KEEFFE,[‡] AND OMAR M. YAGHI^{*†}

Materials Design and Discovery Group, Department of Chemistry, University of Michigan, 930 North University Avenue, Ann Arbor, Michigan 48109-1055, and Department of Chemistry and Biochemistry, Arizona State University, Box 871604, Tempe, Arizona 85287-1604

Received November 13, 2000

ABSTRACT

Secondary building units (SBUs) are molecular complexes and cluster entities in which ligand coordination modes and metal coordination environments can be utilized in the transformation of these fragments into extended porous networks using polytopic linkers (1,4-benzenedicarboxylate, 1,3,5,7-adamantanetetracarboxylate, etc.). Consideration of the geometric and chemical attributes of the SBUs and linkers leads to prediction of the framework topology, and in turn to the design and synthesis of a new class of porous materials with robust structures and high porosity.

Bridging Molecular and Solid-State Chemistry

The construction of extended solids from molecular building blocks is now of great interest due to the advantages it offers for the design of materials. The use of discrete molecular units in the assembly of extended networks is an attractive synthetic approach since it permits reactions to take place at or near room temper-

ature, where the structural integrity of the building units can be maintained throughout the reaction—an aspect that allows for their use as modules in the assembly of extended structures.^{1–18} Molecular modules can be designed to direct the formation of target structures as well as to impart desired physical properties to solid-state materials. In an effort to understand and fully develop this area of chemistry, often termed modular chemistry, a large number of synthetic approaches involving solution assembly of molecules have been pursued to achieve functional mesoscopic phases, modified surfaces, and designed crystals.¹

We have focused on the study of crystalline materials since the attainment of well-defined structures is intimately linked to an understanding of the design, synthesis, and properties of materials. In particular, we have been interested in the construction of porous materials due to their immense impact on the global economy and the fascinating prospects that open networks offer for building complexity into molecular voids in which highly selective inclusion and chemical transformations can be effected. In an earlier Account,⁶ we showed how extended metal–organic frameworks (MOFs) can be designed, crystallized, and fully characterized. Here, we present the next stage in the development of MOFs as a new class of porous materials: the recent progress in using the concept of secondary building units (SBUs) for understanding and predicting topologies of structures, and as synthetic modules for the construction of robust frameworks with *permanent* porosity. We also outline strategies for incorporating unprecedented arrays of coordinatively unsaturated open-metal (OM) sites in porous materials and for the synthesis of modular interpenetrating and non-interpenetrating networks with optimal porosity.

*To whom correspondence should be addressed. E-mail: oyaghi@umich.edu.

[†] University of Michigan.

[‡] Arizona State University.

Mohamed Eddaoudi was born in Agadir, Morocco (1969). He received his B.S. (1991) from the University of Ibnou Zohar with Honors, and M.S. (1992) and Ph.D. (1996) from the University Denis Diderot Paris 7 with *Tres Honorable avec Felicitations du Jury*. He has been a Faculty Research Associate with Professor Yaghi since August 1997. His research focus is on the synthesis, characterization, and inclusion/sorption chemistry of organic and inorganic porous materials.

David B. Moler was born in Ann Arbor, MI (1979). He is a junior student in the Department of Chemical Engineering at the University of Michigan. His interests in chemistry include molecular shapes, topology, and patterns.

Hailian Li was born in Jiangsu, China, in 1964. He received his B.S. (1987) and M.S. (1990) in chemistry from Nanjing University, China. He served as a faculty research associate with Professor Yaghi while at Arizona State University. At present, he is a doctorate candidate at the Department of Chemistry of the University of Michigan. His primary focus is on the synthesis of porous crystalline materials with novel linkages.

Banglin Chen was born in Zhejiang, China (1965). He received his B.S. (1985) and M.S. (1988) from Zhejiang University, and his Ph.D. (1999) from the National University of Singapore. He has been a postdoctoral fellow in Professor Yaghi's group since August 1999. He has invested his efforts in the use of expanded and decorated links for the synthesis of porous materials, in particular interwoven structures.

Theresa M. Reineke was born in St. Paul, MN, in 1972. She received her B.S. degree from the University of Wisconsin-Eau Claire (1995), her M.S. from Arizona State University (1998), and her Ph.D. in inorganic chemistry (2000) from the University of Michigan, Ann Arbor, with Professor O. M. Yaghi. She is currently a Postdoctoral Scholar at the California Institute of Technology with Professor Mark Davis, studying nonviral gene delivery polymers.

Michael O'Keeffe was born in Bury St Edmunds, England (1934). He received his B.Sc. (1954), Ph.D. (1958), and D.Sc. (1976) from the University of Bristol. He is Regents' Professor of Chemistry at Arizona State University, where he has been since 1963. His current research is particularly focused on studying beautiful patterns found in chemistry and elsewhere.

Omar M. Yaghi was born in Amman, Jordan (1965). He received his B.S. in chemistry from the State University of New York-Albany (1985) and his Ph.D. from the University of Illinois-Urbana (1990) with Professor Walter G. Klemperer. From 1990 to 1992, he was an NSF Postdoctoral Fellow at Harvard University with Professor Richard H. Holm. He joined the faculty at Arizona State University in 1992. He was awarded the ACS-Exxon Solid-State Chemistry Award in 1998. In June 1999, he moved to the University of Michigan as a Professor of Chemistry, establishing several research programs dealing with molecular and solid-state chemistry, in particular the transformation of molecular organic and inorganic building blocks to functional extended frameworks.

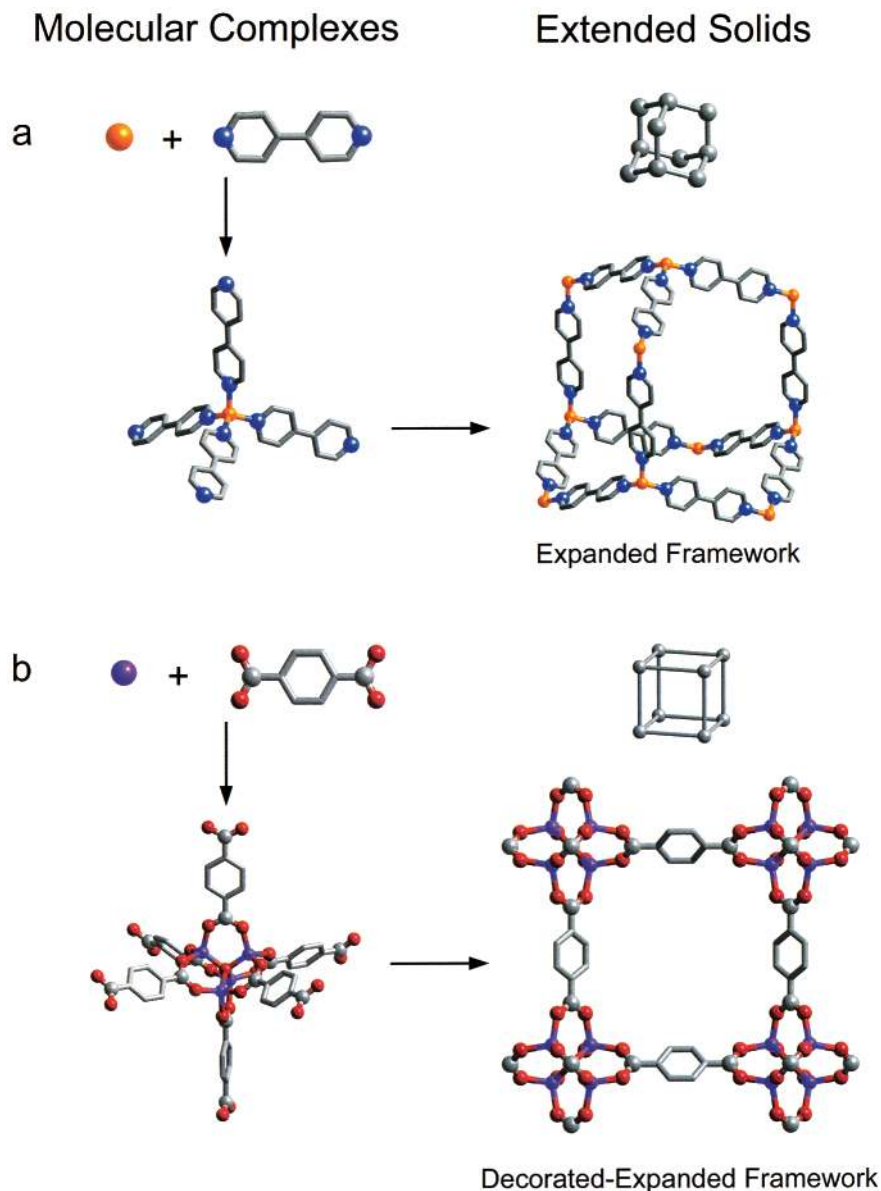


FIGURE 1. Assembly of metal–organic frameworks (MOFs) by the copolymerization of metal ions with organic linkers to give (a) flexible metal–bipyridine structures with expanded diamond topology and (b) rigid metal–carboxylate clusters that can be linked by benzene “struts” to form rigid extended frameworks in which the M–O–C core (SBU) of each cluster acts as a large octahedron decorating a 6-connected vertex in a cube. All hydrogen atoms have been omitted for clarity. (In (a), M, orange; C, gray, N, blue; in (b), M, purple; O, red; C, gray. Structures were drawn using single-crystal X-ray diffraction data.)

Strategies for Construction of Rigid Porous Frameworks

Although synthesis of open frameworks by assembly of metal ions with di-, tri-, and poly-topic N-bound organic linkers such as 4,4'-bipyridine (BPY) has produced many cationic framework structures (Figure 1a), attempts to evacuate/exchange guests within the pores almost invariably, with few exceptions,^{12,15} results in collapse of the host framework. We have found that multidentate linkers such as carboxylates allow for the formation of more rigid frameworks due to their ability to aggregate metal ions into M–O–C clusters that we refer to as secondary building units (SBUs) (Figure 1b). The SBUs are sufficiently rigid because the metal ions are locked into their positions by the carboxylates; thus, instead of having one metal ion

at a network vertex (as is the case in M-BPY compounds), now the SBUs serve as large rigid vertices that can be joined by rigid organic links to produce extended frameworks of high structural stability. The frameworks are also *neutral*, obviating the need for counterions in their cavities.

To appreciate the impact of SBUs on pore size and porosity of frameworks, it is instructive to compare two strategies developed for the construction of highly porous frameworks. (a) The use of long links that increase the spacing between vertices in a net yields void space proportional to the length of linker (Figure 1a). This means that a bond is replaced by a sequence of bonds—a process we call *expansion*. Although in principle such expanded structures provide for large pores, in practice they are

often found to be highly interpenetrated and to have low porosity. (b) In contrast, replacement of a vertex of a framework net by a group of vertices, a process termed *decoration*, results in open structures with high rigidity and without a tendency to interpenetrate (Figure 1b). In fact, when such networks are interpenetrating, optimal pore volume may be achieved as described below. (The replacement of the vertices of an N -connected net by a group of N vertices is a special case of decoration which we refer to as *augmentation*.²⁴)

An increasing number of assembled frameworks have as components polytopic groupings of linkers such as 1,3,5-benzenetricarboxylate (BTB), which in themselves may act to decorate a vertex in an assembly. Polytopic links can thus be employed both to decorate and to expand a net.¹⁴

It is worth noting that the sizes of rings (or pore size) and voids in nets can be significantly increased with decoration, augmentation, or a combination thereof. For example, 4-rings in a simple cubic structure can be augmented by octahedra (carboxylate carbon atoms in Figure 1b, right) to produce a 5-connected structure with 8-ring pores and void space significantly larger than that of the original structure.

From Molecular SBUs to Open Framework Solids

Identification and Use of SBUs. Discrete di-, tri-, and tetranuclear metal carboxylate clusters^{19–23} such as the paddle-wheel copper acetate (D_{4h}) and the basic zinc acetate (T_d) motifs were targeted as symmetrical modules suited for polymerization reactions involving multidentate carboxylate linkers. Such clusters can serve as SBUs in that they have three components relevant to their polymerization into modular porous metal–carboxylate networks (Figure 1b). (a) The M–O–C core structure is an SBU whose shape is defined by those atoms representing points of extension to other SBUs, and which are generally separated only by links. Thus, such atoms define the underlying geometry of the SBU; they are relevant to predicting the overall topology of the modular network (Figure 1b). (b) Potentially, each monocarboxylate ligand in the molecular complex can be substituted with a di-, tri-, or multicarboxylate in order to polymerize the SBU into an extended network. However, the coordination mode of each carboxylate ligand in the molecular complex provides important geometric and conformational information that is critical to predicting the topology of the resulting network. (c) In some clusters where terminal ligands are present, their coordination sites may be removed to allow the study of metal site reactivity: by using weak ligands (such as methanol or ethanol) as solvents in the synthesis, it is possible to produce extended structures in which these ligands point toward the center of the voids, making them susceptible to dissociation and evacuation from the pores, thereby producing periodically arranged OM sites.

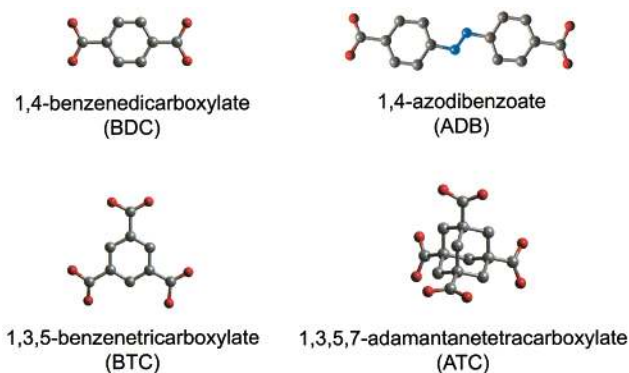


FIGURE 2. Representative polytopic organic linkers. (Same coloring scheme as in Figure 1.)

Solution Synthesis and Crystallization of Modular Porous Solids. Generally, when 3-D extended solids linked by strong chemical bonds are assembled under mild temperature conditions, it is difficult to effect their crystallization, and in general this remains a significant obstacle to synthesis. However, we have developed pathways for synthesizing macrocrystalline modular solids. For example, we have shown that copolymerization of SBUs with the polytopic linkers 1,4-benzenedicarboxylate (BDC), 4,4'-azodibenzoate (ADB), 1,3,5-benzenetricarboxylate (BTC), and 1,3,5,7-adamantanetetracarboxylate (ATC) (Figure 2) is an ideal pathway for obtaining crystalline products. Typically, a solution of the acid form of a linker and the appropriate simple metal salt (nitrate) is prepared in the desired stoichiometry. The key step to obtaining crystals is to *slowly* diffuse into the reaction mixture an organic amine that deprotonates the acid and initiates the assembly. Nucleation rates and the number of nucleation sites can be controlled by controlling the rate of amine diffusion, solvent polarity, and concentration gradients. When the acid is poorly soluble, reactions are performed above room temperature, up to 190 °C. In these cases, inorganic hydroxides such as NaOH may be used (if needed) instead of the organic amines to deprotonate the acid.

Predicting Framework Topologies. A large number of crystalline materials constructed from these SBUs and linkers have been prepared and reported by our group. Illustrative examples involving each SBU mentioned above will be presented. In consideration of possible structures that would form by the polymerization of the SBUs, we rely on our thesis: *in general only a small number of simple, high-symmetry structures will be of overriding general importance, and they would be expected to form most commonly*.²⁴ We know of no systematic survey of the occurrence of structural topologies, and when we say that a particular topology is very common, we really mean that it occurs very frequently in structures that we are likely to have examined and to have analyzed their geometry. Elaboration of this thesis has appeared in a recent tutorial article.²⁴ For the purposes of this presentation, a partial list of structures that are most likely to form in the assembly of certain symmetrical geometric shapes is shown in Table 1 and represented in Figure 3.²⁵ The

Table 1. Partial List of Basic Nets with One or Two Kinds of Vertex Figures^a

coordination	coordination figures		net
3	triangle	triangle	SrSi ₂
3	triangle	triangle	ThSi ₂
3	triangle	triangle	6 ³ honeycomb
3,4	triangle	square	Pt ₃ O ₄
4	square	square	NbO
4	tetrahedron	tetrahedron	diamond (C)
4,4	square	tetrahedron	cooperite (PtS)
4	square	square	4 ⁴ square lattice
6	octahedron	octahedron	primitive cubic
8	cube	cube	body-centered cubic

^a For a more complete list of basic structures, see refs 24 and 25.

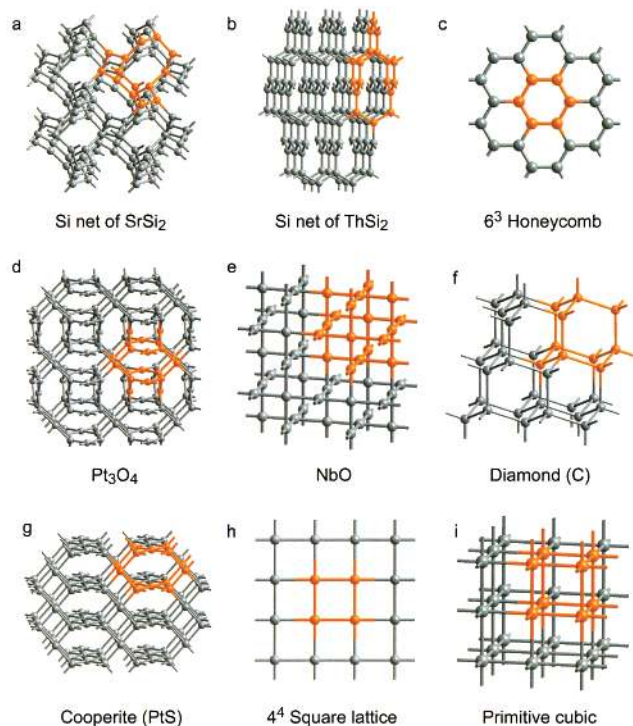


FIGURE 3. Common nets (see Table 1) for one and two kinds of links. A segment of each net has been highlighted in orange for clarity. (Structures were drawn using single-crystal X-ray diffraction data.)

essence of this thesis is captured by discussion of the topologies of extended porous structures prepared from the SBUs discussed above. Unlike other MOFs, these SBUs produce unprecedented porosity due to their rigid structure. A summary of porosity data obtained from gas sorption isotherms is shown in Table 2 and discussed further below.

Design of Periodic Molecular Imprints for Sensing

Decoration and Expansion of Primitive Cubic Net. The trinuclear SBU—known in a molecular cluster²¹—has been polymerized with BDC to form a 3-D porous network, Zn₃(BDC)₃·6CH₃OH (MOF-3) (Figure 4).²⁶ The central zinc atom is octahedrally bound to carboxylate oxygens, and each of the other zinc centers is coordinated to three such oxygens in addition to two oxygens from terminal metha-

Table 2. Comparison of Porosity in MOFs^a

	MOF -2	MOF -3	MOF -4	MOF -5	MOF -6	MOF -9	MOF -11
pore diameter (Å)	7	8	14	12	4	8	7
surface area (m ² /g)	270	140		2900		127	560
pore volume (cm ³ /g)	0.094	0.038	0.612	1.04	0.099	0.035	0.20

^a All parameters were obtained from gas sorption isotherm data. Surface areas for MOF-4 and -6 are not included since these frameworks did not adsorb gases.

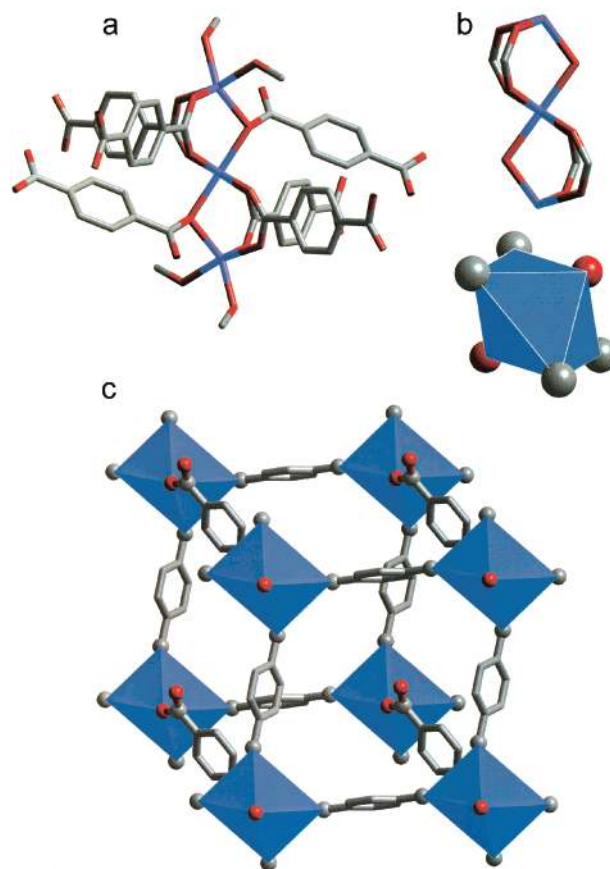


FIGURE 4. (a) Building unit in the crystal structure of Zn₃(BDC)₃·6CH₃OH (MOF-3), in which each carboxylate carbon of four BDC units and an oxygen from each of the remaining BDC links form. (b) Octahedral (Oh) SBU, that assembles into (c) a primitive cubic-like decorated diamond net topology. (Same coloring scheme as in Figure 1; structures were drawn using single-crystal X-ray diffraction data.)

nol ligands, where one methanol is bound more weakly to zinc than the other (Figure 4a). In the crystal, two additional methanol molecules are hydrogen bonded to the methanol ligands, thus acting as guests to fill a 3-D channel system of 8 Å cross section.

To determine the topology of MOF-3 based on the guidelines presented above, each trinuclear unit can be considered as an octahedral SBU (Figure 4b). Linking these units with BDC produces the primitive cubic net arrangement (Table 1, Figure 3i): the octahedral SBU decorates the vertices that are then spaced (expanded) from other such units by 2-connected benzene units (in

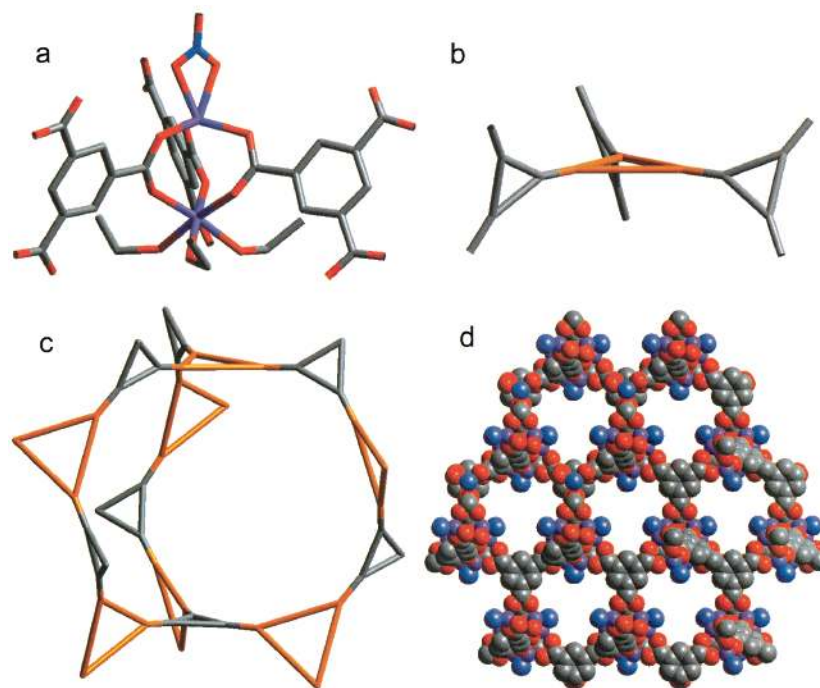


FIGURE 5. (a) Building unit in the crystal structure of $\text{Zn}_2(\text{BTC})(\text{NO}_3) \cdot (\text{C}_2\text{H}_5\text{OH})_5(\text{H}_2\text{O})$ (MOF-4) having terminal ethanol and nitrate ligands bound to opposite zinc centers. The carboxylate carbon atoms within each $\text{M}-\text{O}-\text{C}$ cluster core and the 1,3,5-carbon atoms of each BTC represent (b) two triangle SBUs (respectively shown in orange and gray), which assemble (c) into decorated Si net of SrSi_2 , to form (d) an extended porous framework with open metal sites and large pores. (Same coloring scheme as in Figure 1; structures were drawn using single-crystal X-ray diffraction data.)

the case of BDC having one carboxylate oxygen as part of the SBU, the expansion is done with a benzyl unit) (Figure 4c).

We found that all methanol, including the ligands, can be removed from the voids to give a porous network (Table 2) having open zinc sites. It is interesting to note that MOF-3 maintains its framework integrity, even in the absence of methanol guests or ligands—an aspect that is relevant to sensing and catalysis.²⁷ In the following sections, we give examples that illustrate how the OM sites can act as molecular imprints.

A Chiral Framework with Imprinted Crevices. A cubic network with larger pores and with OM sites can be achieved using the common dinuclear cluster $D_{3h}\text{-Zn}_2(\text{CO}_2)_3$.²⁰ Copolymerization of BTC with zinc(II) yields a building unit with a trigonal SBU geometry (Figure 5a) in which the carbon atoms of the $\text{Zn}-\text{O}-\text{C}$ cluster core are the vertices of a trigonal SBU and three carbon atoms of the benzene rings of BTC are the vertices of another trigonal SBU (Figure 5b). This arrangement yields $\text{Zn}_2(\text{BTC})(\text{NO}_3) \cdot (\text{C}_2\text{H}_5\text{OH})_5(\text{H}_2\text{O})$ (MOF-4),²⁸ which adopts one of the most symmetric and frequently observed 3-connected topologies belonging to the set summarized in Table 1, namely the chiral Si net of SrSi_2 (Figure 3a).^{24,25} Here, each SBU and benzene unit alternately decorates the Si vertices (Figure 5c).

Each building unit has a nitrate ion bound strongly to one of the Zn centers and three ethanol molecules bound weakly to the other Zn center. The crystal structure of MOF-4 is cubic and contains 3-D channels of 14 Å diameter filled with five ethanol (three act as ligands to

Zn and two are free guests filling the pores) and one water molecule per formula unit. Using liquid and vapor sorption, it was shown that all ethanol and water can be evacuated from the pores to produce pyramidal Zn sites that are found to be highly selective to alcohol uptake.²⁹ Guest competition experiments using ^{13}C CPMAS NMR, GC, and liquid isotherms showed that when evacuated MOF-4 is exposed to an equimolar mixture of CH_3CN and CH_3OH , only CH_3OH is allowed into the pores. Similar experiments involving larger molecules produced similar affinity of the pores to alcohols. This has led us to conclude that the exposed zinc sites are part of a crevice left behind by the liberated ethanol, where a geometric and electronic imprint (specific host–guest hydrogen-bonding interactions) for alcohols has been registered at the binding sites (Figure 5d).²⁹

Design and Crystal Structure of Materials with Open Metal Sites

Decorated Square Grids. The paddle-wheel cluster is known in many complexes;¹⁹ it has a square geometry (Figure 6a), which when linked with benzene, a linear ditopic “strut”, produces $\text{Zn}(\text{BDC})(\text{H}_2\text{O}) \cdot (\text{DMF})$ (MOF-2); DMF = *N,N'*-dimethylformamide) having a layered structure.³² Here, $\text{Zn}_2(\text{CO}_2)_4$ square SBUs decorate the intersection of a 4⁴ planar grid, and the benzene units expand the links between vertices to produce the 4.8² tiling pattern (Figure 6b). The axial positions on Zn are occupied by water ligands which serve to hold together the sheets by mutual hydrogen bonding to the carboxylate oxygen on

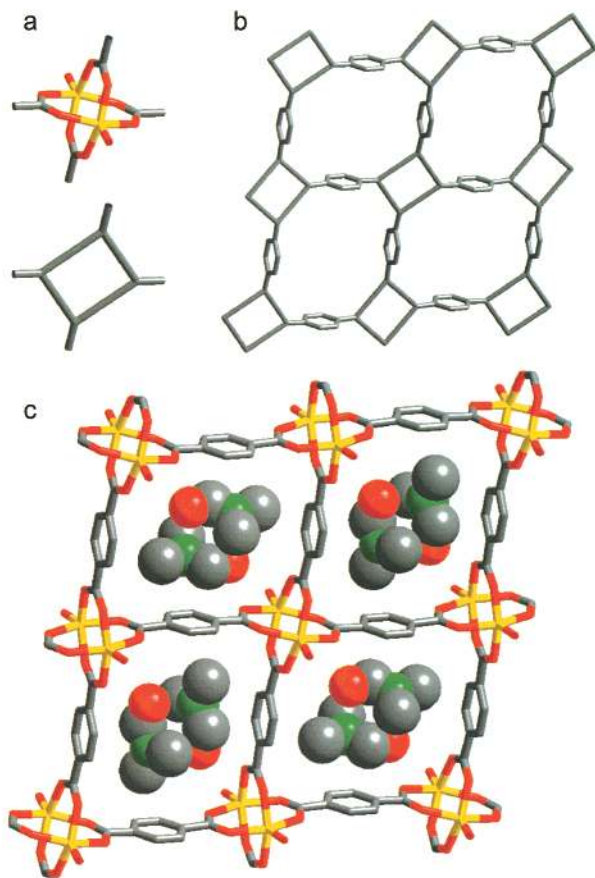


FIGURE 6. (a) Paddle-wheel cluster, a square SBU, which is the building unit in the crystal structure of $\text{Zn}(\text{BDC})(\text{H}_2\text{O})\cdot(\text{DMF})$ (MOF-2), which forms (b) a decorated square grid and (c) an open framework with DMF occupying the pores. (Zn, yellow; O, red; N, green; C, gray. Structures were drawn using single-crystal X-ray diffraction data.)

an adjacent sheet. The sheets stack in registry to allow the formation of 1-D channels where DMF guests reside (Figure 6c). The DMF and water can be thermally removed to allow each metal to bond to a carboxylate oxygen of an adjacent sheet, thereby linking the sheets in the third dimension and leading to a quasi 3-D network with open channels. The porosity of this material was examined and found to exhibit zeolite-like type I gas sorption isotherms (Table 2).³²

Porous Crystals with Open Metal Sites. It is well-known that when the axial ligands in the paddle-wheel structure have been dissociated, as in MOF-2, the metal sites thus produced bind to a Lewis base atom on a neighboring unit to give polymeric structures having no OM sites.³³ Our strategy to prevent coupling of these units and to achieve an MOF with accessible OM sites relies on using the square SBU with a tetrahedral linker. Using the organic adamantane cluster as a second SBU, we expected that the combination of a square (Figure 7a,b) and a tetrahedron would polymerize to form the PtS topology, as indicated in Table 1 (Figure 3g). Here, each square Pt atom and tetrahedral S atom in PtS would be replaced by an inorganic square and an organic tetrahedral SBU, respectively, to give a decorated form of PtS (Figure 7c). Indeed, the success of this approach has been

demonstrated by performing reactions that give the copper carboxylate square motif: addition of $\text{Cu}(\text{NO}_3)_2\cdot 2.5\text{H}_2\text{O}$ to 1,3,5,7-adamantanetetracarboxylic acid (H_4ATC) in basic aqueous solution at 190 °C yields green crystals of $\text{Cu}_2(\text{ATC})\cdot 6\text{H}_2\text{O}$ (MOF-11) having the desired geometry in which self-aggregation of SBUs is prevented since the labile ligands point toward the centers of voids (Figure 7d).³⁴ Each square has two axial water ligands ($\text{Cu}-\text{OH}_2 = 2.148(3) \text{ \AA}$), one bound to each of its copper(II) centers. These point away from the $\text{Cu}-\text{O}-\text{C}$ framework into a 3-D channel system of 6.0–6.5 Å diameter, where four additional water guests per square unit reside. Estimates based on van der Waals radii showed that water ligands and guests occupy approximately 50% of the crystal volume. All water guests and ligands were liberated to give an anhydrous framework with a thermal stability range 120–260 °C. Furthermore, the rigid and porous nature of the anhydrous framework was evident upon measurement of its gas sorption isotherms, where fully reversible type I behavior was observed for $\text{N}_{2(\text{g})}$ and $\text{Ar}_{(\text{g})}$ —unequivocally confirming the existence of permanent porosity in anhydrous MOF-11 (Table 2).

The crystal structure of the anhydrous material (Figure 7d) showed that the originally monoclinic framework relaxes to the tetragonal symmetry of the ideal PtS net with negligible change in volume (Table 3). The absence of water ligands on copper is evident from the shorter distance observed for $\text{Cu}-\text{OCO}$ and a significant shortening of the $\text{Cu}-\text{Cu}$ distance upon liberation of water—the latter (2.490 Å) being the shortest distance known for copper(II) carboxylate compounds. Magnetic susceptibility data obtained for the as-synthesized MOF-11 follow the expected behavior typically observed for antiferromagnetic coupling in the copper(II) acetate dimer ($2J = -280 \text{ cm}^{-1}$); however, the anhydrous material showed increased coupling ($2J = -444 \text{ cm}^{-1}$), as expected for the observed shortening of the $\text{Cu}-\text{O}$ distance found in the X-ray crystal diffraction analysis.

The full characterization of the OM sites in MOF-11 paves the way for their use in sensors, in catalysis, and as functionalization sites for mounting molecular moieties into the pores. An example of the potential use of OM sites in sensing is presented in the section that follows.

Luminescent Porous Frameworks. To examine the viability of MOFs with OM sites in sensing small molecules, we initiated a project aimed at exploring the chemistry of frameworks with lanthanide metal ions. It was shown that the compound $\text{Tb}_2(\text{BDC})_3\cdot(\text{H}_2\text{O})_4$ (MOF-6), which has an extended nonporous structure, can be converted to a porous network, $\text{Tb}_2(\text{BDC})_3$, by thermally liberating the water ligands (Table 2).³⁰ The dehydrated form has extended 1-D channels and the same framework structure as that of the as-synthesized solid, as shown by X-ray powder diffraction. Water sorption isotherm data proved that $\text{Tb}_2(\text{BDC})_3$ has permanent porosity and accessible Tb(III) sites. Luminescence lifetime measurements confirmed that when water is resorbed or ammonia is sorbed into the pores, they bind to Tb, giving distinctly different decay luminescence lifetime constants. Further

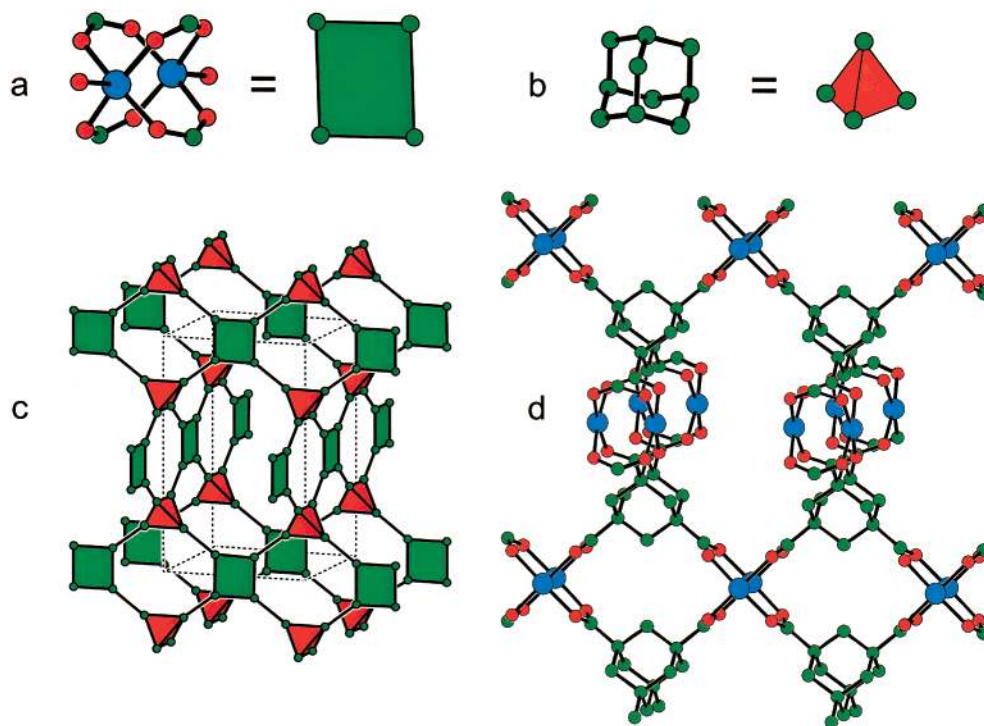


FIGURE 7. (a) Paddle-wheel $\text{Cu}_2(\text{OCO})_4$ SBU (Cu, blue; C, green; O, red) of square geometry (green) and (b) adamantane SBU (C, green) of tetrahedral geometry (red). These building blocks assemble to adopt the PtS net with its vertices occupied by the clusters to form (c) a decorated PtS framework, where (d) open metal sites point into the pores (same color scheme as in (a) and (b)). (Structures were drawn using single-crystal X-ray diffraction data.)

Table 3. Crystallographic Data and Important Interatomic Distances for MOF-11

crystals, chemical formula	crystal system, space group	unit cell: a, b, c (Å); α, β, γ (°)	V (Å ³)	Z	$R1$ ($I > 2\sigma(I)$)	Cu–OCO distance (Å)	Cu–Cu distance (Å)
as-synthesized $\text{Cu}_2(\text{ATC}) \cdot 6\text{H}_2\text{O}$	monoclinic, $C2/c$	$a = 8.5732^a$ $b = 8.5732$ $c = 14.3359$ $\alpha = 93.92$ $\beta = 87.08$ $\gamma = 98.27$	1040.4(1)	2 ^a	0.0433	1.976(2) 1.989(2) 1.964(2)	2.622(3)
dehydrated $\text{Cu}_2(\text{ATC})$	tetragonal, $P4_2/mmc$	$a = 8.4671(2)$ $b = 8.4671(1)$ $c = 14.444(1)$	1035.5(1)	2	0.0353	1.935(2)	2.490(3)

^a Primitive cell. The conventional C-centered cell has $a = 12.98658(2)$, $b = 11.2200(1)$, and $c = 11.3359(2)$ Å, $\beta = 93.857(1)^\circ$, $Z = 4$.

work along these lines has produced another framework with larger pores that potentially may exhibit more diverse luminescent properties.³¹

Beyond Zeolites: MOFs with High Porosity and Stability

MOF-5. The basic zinc acetate structure²² can be extended into a 3-D network with BDC to give $\text{Zn}_4\text{O}(\text{BDC})_3 \cdot (\text{DMF})_8 \cdot (\text{C}_6\text{H}_5\text{Cl})$ (MOF-5), a simple cubic 5-connected net, as indicated in Table 1 (Figure 8a,b): the nodes (vertices) of the cubic net are replaced by octahedral SBUs, and the links (edges) of the net are replaced by finite rods of BDC atoms.³⁵ The pores are a 3-D channel system of 8 Å aperture and 12 Å cross section filled with eight DMF SBUs and one chlorobenzene SBU (Figure 8c). The guests can be easily exchanged or/and evacuated from the pores without loss of the framework integrity.

To evaluate the pore volume and the apparent surface area of this framework (Table 2), the gas and vapor sorption isotherms for the desolvated sample were measured. $\text{N}_{2(g)}$ sorption revealed a reversible type I isotherm (Figure 9). The same sorption behavior was observed for $\text{Ar}_{(g)}$ and organic vapors such as CH_2Cl_2 , CHCl_3 , CCl_4 , C_6H_6 , and C_6H_{12} . Similar to those of most zeolites, the isotherms are reversible and show no hysteresis upon desorption of gases from the pores. The apparent Langmuir surface area was estimated at 2900 m²/g. Typically for crystalline zeolites, which generally have higher molar mass than $\text{Zn}_4\text{O}(\text{BDC})_3$, surface areas ranging up to 500 m²/g are found.

Crystal Structure of MOF-5 with Completely Empty Channels. At the outset of this work, the porosity of MOFs was unexamined, leaving doubts as to whether such frameworks were viable as porous materials—a question of considerable interest. Starting with MOF-2, we showed

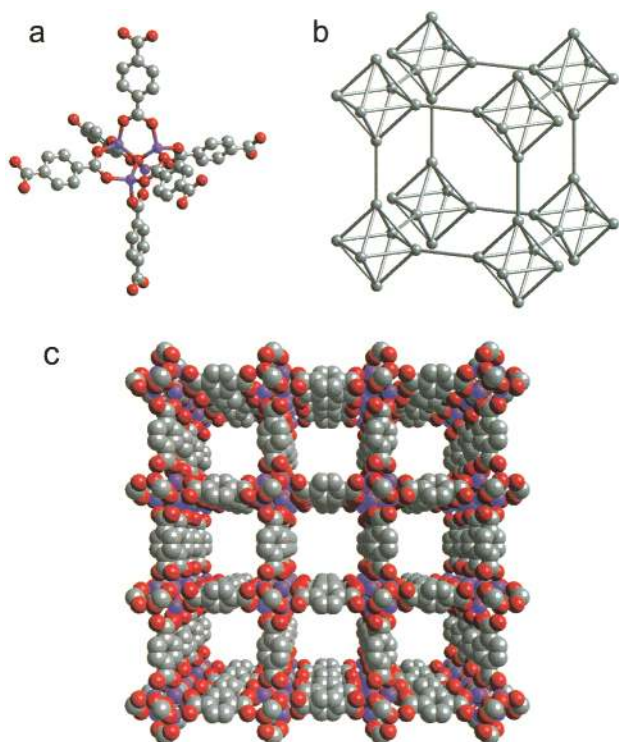


FIGURE 8. (a) Building unit present in crystals of $\text{Zn}_4\text{O}(\text{BDC})_3 \cdot (\text{DMF})_8$ ($\text{C}_6\text{H}_5\text{Cl}$) (MOF-5), where the carboxylate carbon atoms are in an octahedral geometry decorating (b) a primitive cubic lattice, and form (c) the most porous crystals known to date. (Same coloring scheme as in Figure 1; structures were drawn using single-crystal X-ray diffraction data.)

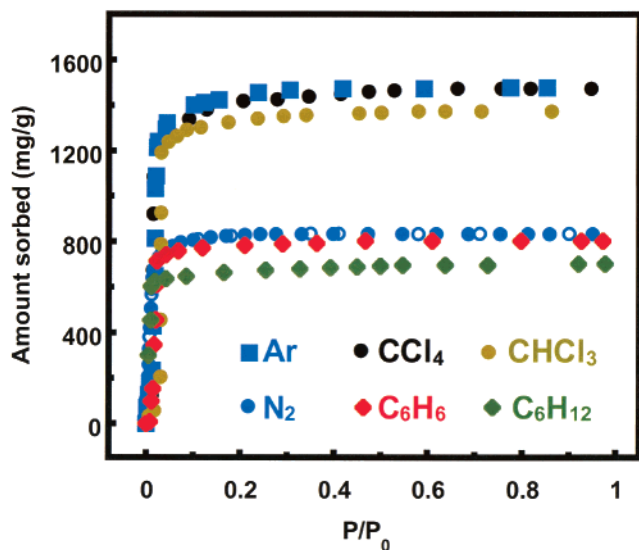


FIGURE 9. Typical gas sorption isotherms for MOFs, shown here for MOF-5.

that modular MOFs prepared from metal carboxylates can be constructed with sufficient rigidity and structural stability to support permanent porosity in the absence of guests. Since then, we have shown numerous other examples of MOFs that exhibit zeolite-like gas sorption isotherms.

Much of the early work has been subject to one or more of the following criticisms. (a) The crystal structures are

unreliable because disorder of the guests leads to large R values. (b) The guests cannot be completely removed from the pores without collapse of the framework. (c) Crystal structures of empty frameworks with significant porosity have not been reported. In this section we show that it is possible to obtain the crystal structure of a highly porous framework, where the guests have been removed from the channels and the crystals placed under vacuum.

In an influential paper, Harlow³⁶ identifies several classes of crystal structures, two of which concern us here. (a) *Quality structures*: for an organometallic structure it is stated that if the hydrogen atoms can be refined with C–H distances between 0.85 and 1.05 Å and isotropic atom displacement parameter, B , less than 6 Å², “the data must be of high quality and the model must be correct”. (b) At the other extreme come *junk structures*. These have large R values; it is suggested that for $R > 0.15$, “there are no useful lessons to be learned from them”. For those interested in constructing highly porous metal–organic networks, the great majority of such structures published to date fall more nearly into the second category, and there is a continuing debate as to their reliability.

In the cubic porous material, $\text{Zn}_4\text{O}(\text{BDC})_3$ (MOF-5), discussed above, the DMF and chlorobenzene guests in the cavities of the as-synthesized form of MOF-5 are disordered and could not be refined in the original structure determination, and the resulting crystal structure had $R_1 = 0.11$ (Table 4). Direct evidence for the striking stability of the framework was obtained by evacuating the pores and performing a structure determination on the desolvated crystals which showed that the cell parameters were virtually unchanged. In addition, heating the fully desolvated crystals in air at 300 °C for 24 h had no impact on either their morphology or their crystallinity, as evidenced by another X-ray single-crystal diffraction study. Here, again, the cell parameters obtained were virtually unaltered from those found for the unheated desolvated crystals. We subsequently found that crystal integrity is maintained even when the crystal is placed in vacuo. A structure determination, which refined to $R = 0.019$ (see Tables 4 and 5), was carried out on the crystal placed under vacuum. The H atoms of the BDC groups refined to give a carbon–hydrogen bond length of 0.93(3) Å and $B = 5.5$ Å². The maximum peak in the final difference map was 0.2 e[−] Å^{−3}, showing that the channels in the structure were really empty.

It is worth noting that by Harlow’s criteria we have gone from close to a “junk structure” to a “quality structure”. It is therefore of considerable interest to compare the two structures, as is done in Tables 4 and 5. The structures are generally in excellent agreement but have esd’s about 10 times larger for the solvated sample. This translates into errors for non-hydrogen bond lengths being as much as 0.03 Å for the solvated structure compared to <0.004 Å for the evacuated sample. However, apart from the difference in esd’s, the structures are essentially identical.

It is important to recognize that the evacuated structure of MOF-5 is, we believe, the most porous crystal structure

Table 4. Crystal Data for MOF-5

	Zn ₄ O(BDC) ₃ · (DMF) ₈ (C ₆ H ₅ Cl) as synthesized	Zn ₄ O(BDC) ₃		
		fully desolvated	300 °C for 24 h in air	vacuum
<i>T</i> (K)	213 ± 2	169 ± 2	149 ± 2	165 ± 2
space group	<i>Fm</i> 3 <i>m</i>	<i>Fm</i> 3 <i>m</i>	<i>Fm</i> 3 <i>m</i>	<i>Fm</i> 3 <i>m</i>
<i>a</i> (Å)	25.6690(3)	25.8849(3)	25.8496(3)	25.8556(3)
<i>Z</i>	8	8	8	8
<i>V</i> (Å ³)	16 913.2(3)	17 343.6(3)	17 272.7(3)	17 284.8(3)
ρ (g/cm ³)	1.2	0.59	0.59	0.59
<i>R</i> , <i>R</i> _w	0.11, 0.31	0.023, 0.026		0.019/0.024
max./min. (e [−] /Å ³)	1.56/−0.45	0.25/−0.17		0.20/−0.30

Table 5. Comparison of Atomic Coordinates for As-Synthesized (Solvated) and Evacuated (Vacuum) MOF-5

atom	compound	<i>x</i>	<i>y</i>	<i>z</i>	<i>B</i> (Å ²)
Zn	vacuum	0.293477(7)	<i>x</i>	<i>x</i>	1.714(2)
	solvated	0.2935(1)	<i>x</i>	<i>x</i>	4.0(1)
C1	vacuum	0.11146(10)	1/4	1/4	2.53(3)
	solvated	0.1105(7)	1/4	1/4	6.9(2)
C2	vacuum	0.05386(10)	1/4	1/4	2.75(3)
	solvated	0.0538(7)	1/4	1/4	7.7(6)
C3	vacuum	0.21751(6)	<i>x</i>	0.47343(8)	4.11(3)
	solvated	0.2169(4)	<i>x</i>	0.4737(6)	9.7(6)
O1	vacuum	1/4	1/4	1/4	3.08(2)
	solvated	1/4	1/4	1/4	3.3(4)
O2	vacuum	0.21937(4)	<i>x</i>	0.36611(5)	1.63(1)
	solvated	0.2182(3)		0.3661(4)	7.6(3)
H1	vacuum	0.1956(7)	<i>x</i>	0.45520(1)	5.5(7)
	solvated	0.1941	<i>x</i>	0.4548	11.7

ever determined; certainly it is one of the least dense (of crystalline materials stable at room temperature and pressure, metallic lithium appears to be the only one less dense). The density of the evacuated crystal is 0.59 Mg m^{−3}, compared with 1.14 Mg m^{−3} for the solvated crystal. This study confirmed for the first time that, with a stable and rigid framework such as that of MOF-5, permanent porosity exists even in the absence of guests and that the structure of the evacuated framework can be determined with high accuracy by single-crystal diffraction techniques. It also showed that, although crystal structures of open structures with disordered guest molecules and other species have high *R* values, the positions of the framework atoms can be determined reliably—a point of some dispute in the past.

The Role of SBUs in Catenation: Achieving Optimal Porosity

Interpenetration. The Tb₂C₄O₈ core units (already known in molecular clusters)²³ can be employed as an octahedral SBU (Figure 10 a,b). This SBU is copolymerized with the long dicarboxylate linker ADB to produce Tb₂(ADB)₃·[(CH₃)₂SO]₂₀ (MOF-9), in which an additional bidentate carboxylate is bound to each Tb; however, the octahedral topology of the SBU is still preserved. Crystals of MOF-9 have a doubly interpenetrating structure with each framework having an idealized simple cubic 6-connected net (Figure 10c).³⁷ Despite the presence of two interpenetrating networks, at least 20 DMSO guest molecules per SBU occupy the pores (Table 2), or a volume representing 71% of the crystal volume, a value greater than previously observed for interpenetrating structures. To explain this

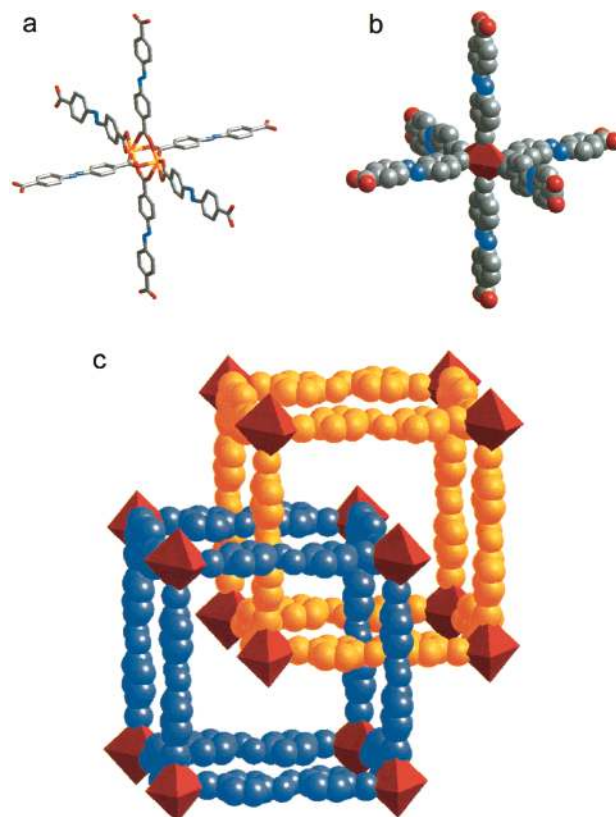


FIGURE 10. Crystal structure of MOF-9 (shown at 45° from the *ab* plane) constructed from (a) approximately octahedral Tb₂(ADB)₃·(DMSO)₄ building units (Tb, orange; O, red; C, gray; N, blue) with the DMSO ligands (two on each Tb atom) not shown. A representation of this SBU is shown in (b) as an octahedron linked to ADB (space filling). This gives (c) two interpenetrating networks (colored separately in blue and orange) with large void space.

unusually large void space in a *maximally* interpenetrating network, we considered a simple geometric argument involving spherical SBUs of diameter *d* that form a primitive cubic network with linkers of length *l*. The cubic cell edge is *a* = *d* + *l*. If the van der Waals diameter (δ) of the atom joining the SBU and linker is considered, then for *n* frameworks to interpenetrate with centers of the SBUs aligned along a body diagonal, $n(d + \delta) \leq 3^{1/2}a$; thus, $n \leq 3^{1/2}(d + l)/(d + \delta)$.

A composite plot (Figure 11) of *n* as a function of *d* and *l* and their relationship to the free volume is used to gain insight into interpenetrating structures. The plot clearly shows that the level of interpenetration is predominantly determined by the length of linkers, *l*, while the free volume is largely influenced by the size of the

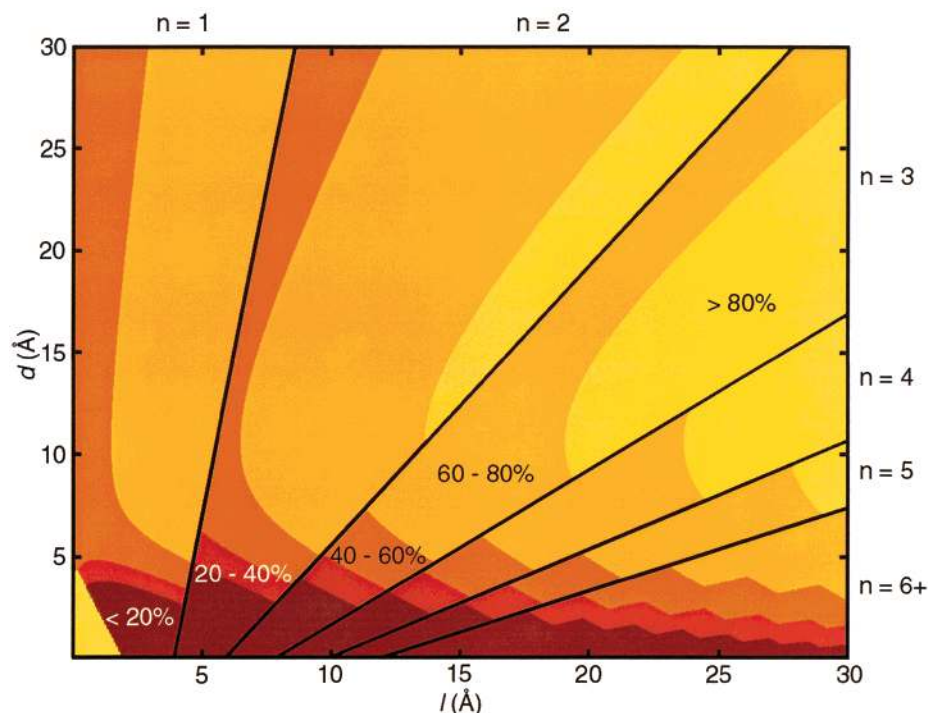


FIGURE 11. A d – l – n – v plot for a cubic system having spherical SBUs and cylinder-shaped rods: n is plotted (total number of frameworks in a structure) as a function of d (diameter of an SBU) and l (length of linker), with the corresponding free volume expressed as the percent of crystal volume shown in decreasing shades of darkness (darkest, <20, to lightest, >80%).

SBUs, d . Significantly, for structures having a small degree of interpenetration ($n = 2$ or 3 in the example here), an optimum amount of available free volume can be achieved. Also, due to the use of bulky SBUs, structures having large free volume are possible at an even higher level of interpenetration ($n \geq 4$). Furthermore, the free volume becomes smaller at high degrees of interpenetration (with relatively small SBUs) because now much of the available space is taken up by the linkers.

The case of MOF-9 can be considered here although it is not strictly cubic: we find that $d = 9.65$ Å and $l = 11.88$ Å, which lies in the region of $n = 2$ with void volume of 60–80%. Note that if d were shorter by only 2 Å, then a structure having three interpenetrating frameworks with less free volume (40%) would be expected (Figure 11). Thus, the Tb–O–C cluster served as an optimal SBU for ADB, allowing MOF-9 to just miss having a third interpenetrating framework. It should be noted that although large porosity can be achieved for a given structure, the pore aperture is completely dependent on the diameter of the SBU. Nevertheless, it should be possible to access apertures in the micro- and mesoporous regimes using ordinary SBUs and organic links.

Interweaving. The structures most commonly found interpenetrating are based on the SrSi_2 , diamond, and simple cubic nets. In these cases a net and its interpenetrating partner are maximally displaced from the periodic surfaces (the G, D, and P minimal surfaces,³⁸ respectively) that separate them. However, the vertices of the most symmetrical (3,4)-connected net, that named for Pt_3O_4 ^{24,25} (cf. Table 1), lie on the cubic P surface. In the structure with a second interpenetrating net (displaced from the

first by $1/2, 1/2, 1/2$) the 4-connected vertices, all on the same surface, avoid each other, but the 3-connected vertices superimpose. However, the 3-connected vertices can be symmetrically displaced from the surface to produce an interwoven structure. We refer to the resulting structure as “interwoven” rather than “interpenetrating” as the two nets reinforce each other while the cavities of each net superimpose and remain empty. We have recently¹⁴ exploited this principle to prepare two interwoven Pt_3O_4 nets in which the square SBU is again the Cu_2 paddle-wheel and the tritopic linker is 1,3,5-benzenetribenzoate (BTB). The resulting cubic framework with composition $\text{Cu}_2(\text{BTB})_3 \cdot (\text{H}_2\text{O})_2$ is remarkably robust and has the largest accessible pores (16.4 Å diameter) yet found in a material of this kind.

Concluding Remarks

It has now been demonstrated that a new class of crystalline porous materials (MOFs) have been synthesized and fully characterized. The ability to design their structures has allowed the synthesis of compositions with designed pore structure (size, shape, and function) and porosity—aspects well beyond what has been achieved with the most porous zeolites and related oxide molecular sieves. The successful use of secondary building units in the formation of certain predicted structures and its impact on identifying networks with optimal porosity is evidence that chemists are at a stage where the primary backbone of extended structures (linked by strong bonds) can be designed.

Establishing porosity in MOFs as illustrated by the successful single-crystal structure analysis of fully *evacuated* frameworks and gas sorption isotherms constitutes an important step in extending the concepts of design toward addressing outstanding challenges. Namely, (a) the important one of functionalizing the pores with useful molecular moieties that introduce weaker and reversible interactions (complex function) into such open frameworks, (b) the assembly and use of less symmetric SBUs, including chiral ones, and (c) the design of dimensionally larger SBUs that still have a small number (3–6) of points of connection allowing them to be incorporated into open frameworks. Current work in this group is focused on addressing these challenges and on pursuing the applications of these materials in catalysis, gas and liquid separations, methane and hydrogen storage, and luminescence-based sensors.

The authors acknowledge the contributions of our colleagues cited in the references and support from the National Science Foundation (DMR-9980469 and DMR-9804817) and the Department of Energy.

References

- (1) *Modular Chemistry*; Michl, J., Ed.; Kluwer Academic Publishers: Dordrecht, 1995, and references therein.
- (2) Bowes, C. L.; Ozin, G. A. Self-Assembling Frameworks: Beyond Microporous Oxides. *Adv. Mater.* **1996**, *8*, 13–28.
- (3) Cheetham, A. K.; Férey, G.; Loiseau, T. Open-Framework Inorganic Materials. *Angew. Chem., Int. Ed.* **1999**, *28*, 3268–3292.
- (4) Hargman, P. J.; Hargman, D.; Zubietta, J. Organic–Inorganic Hybrid Materials: From “Simple” Coordination Polymers to Organodiamine-Templated Molybdenum Oxides. *Angew. Chem., Int. Ed.* **1999**, *38*, 2638–2684.
- (5) Stein, A.; Keller, S. W.; Mallouk, T. E. Turning Down the Heat: Design and Mechanism in Solid-State Synthesis. *Science* **1993**, *259*, 1558–1564.
- (6) Yaghi, O. M.; Li, H.; Davis, C.; Richardson, D.; Groy, T. L. Synthetic Strategies, Structure Patterns, and Emerging Properties in the Chemistry of Modular Porous Solids. *Acc. Chem. Res.* **1998**, *31*, 474–484.
- (7) Hennigar, T. L.; MacQuarrie, D. C.; Losier, P.; Rogers, R. D.; Zaworotko, M. J. Supramolecular Isomerism in Coordination Polymers: Conformational Freedom of Ligands in $[\text{Co}(\text{NO}_3)_2(1,2\text{-bis}(4\text{-pyridyl)ethane})_{1.5}]_n$. *Angew. Chem., Int. Ed. Engl.* **1997**, *36*, 972–973.
- (8) Batten, S. R.; Robson, R. Interpenetrating Nets: Ordered, Periodic Entanglement. *Angew. Chem., Int. Ed.* **1998**, *37*, 1460–1494.
- (9) Kitagawa, S.; Kondo, M. Functional Micropore Chemistry of Crystalline Metal Complex-Assembled Compounds. *Bull. Chem. Soc. Jpn.* **1998**, *71*, 1739–1753.
- (10) Blake, A. J.; Champness, N. R.; Hubberstey, P.; Li, W.-S.; Withersby, M. A.; Schröder, M. Inorganic Crystal Engineering Using Self-Assembly of Tailored Building-Blocks. *Coord. Chem. Rev.* **1999**, *183*, 117–138.
- (11) Lu, J.; Paliwala, T.; Lim, S. C.; Yu, C.; Niu, T.; Jacobson, A. J. Coordination Polymers of $\text{Co}(\text{NCS})_2$ with Pyrazine and 4,4'-Bipyridine: Syntheses and Structures. *Inorg. Chem.* **1997**, *36*, 923–929.
- (12) Biradha, K.; Hongo, Yoshito, H.; Fujita, M. Open Square-Grid Coordination Polymers of the Dimensions $20 \times 20 \text{ \AA}$: Remarkably Stable and Crystalline Solids Even after Guest Removal. *Angew. Chem., Int. Ed.* **2000**, *39*, 3843–3845.
- (13) Xiong, R.-G.; Wilson, S. R.; Lin, W. Bis(Isonicotinato)Iron(II): A Rare, Neutral Three-Dimensional Iron Coordination Polymer. *J. Chem. Soc., Dalton Commun.* **1998**, 4089–4090.
- (14) Chen, L.; Eddaoudi, M.; Hyde, S. T.; O'Keeffe, M.; Yaghi, O. M. Interwoven Metal-Organic Framework on a Periodic Minimal Surface with Extra-Large Pores. *Science* **2001**, *291*, 1021–1023.
- (15) Kepert, C. J.; Rosseinsky, M. J. Zeolite-Like Crystal Structure of an Empty Microporous Molecular Framework. *Chem. Commun.* **1999**, 375–376.
- (16) Goodgame, D. M. L.; Grachvogel, D. A.; Williams, D. J. A New Type of Metal-Organic Large-Pore Zeotype. *Angew. Chem., Int. Ed.* **1999**, *38*, 153–156.
- (17) Carlucci, L.; Ciani, G.; Proserpio, D. M. Interpenetrated and Noninterpenetrated Three-Dimensional Networks in the Polymeric Species $\text{Ag}(\text{tta})$ and $2 \text{ Ag}(\text{tta}) \cdot \text{AgNO}_3$ (tta=tetrazolate): The First Examples of the $\mu_4\text{-}\eta^1\text{:}\eta^1\text{:}\eta^1\text{:}\eta^1$ Bonding Mode for Tetrazolate. *Angew. Chem., Int. Ed.* **1999**, *38*, 3488–3492.
- (18) Kiang, Y.-H.; Gardner, G. B.; Lee, S.; Xu, Z.; Lobkovsky, E. B. Variable Pore Size, Variable Chemical Functionality, and an Example of Reactivity within Porous Phenylacetylene Silver Salts. *J. Am. Chem. Soc.* **1999**, *121*, 8204–8215.
- (19) Clegg, W.; Little, I. R.; Straughan, B. P. Zinc Carboxylate Complexes: Structural Characterisation of Some Binuclear and Linear Trinuclear Complexes. *J. Chem. Soc., Dalton Trans.* **1986**, 1283–1288.
- (20) Malik, M. A.; Motevalli, M.; O'Brien, P. Structural Diversity in the Carbamate Chemistry of Zinc: X-ray Single-Crystal Structures of $[(\text{Me}_2\text{NCH}_2)_2\text{Zn}(\text{O}_2\text{CN}(\text{C}_2\text{H}_5)_2)_2]$ and $[\text{C}_6\text{H}_5\text{NZNMe}(\text{O}_2\text{CN}(\text{C}_2\text{H}_5)_2)_3]$. *Inorg. Chem.* **1995**, *34*, 6223–6225.
- (21) Clegg, W.; Little, I. R.; Straughan, B. P. Preparation and Crystal Structure of a Carboxylate-bridged Linear Trinuclear Zinc(II) Complex. *J. Chem. Soc., Chem. Commun.* **1985**, 73–74.
- (22) Clegg, W.; Harbron, D. R.; Homan, C. D.; Hunt, P. A.; Little, I. R.; Straughan, B. P. Crystal Structures of Three Basic Zinc Carboxylates Together with Infrared and FAB Mass Spectrometry Studies in Solution. *Inorganica Chimica Acta* **1991**, *186*, 51–60.
- (23) Kuz'mina, N. P.; Martynenko, L. I.; Tu, Z. A.; Nguet, C. T.; Troyanov, S. I.; Rykov, A. N.; Korenev, Y. M. Rare-Earth(III) Pivalates. *Russ. J. Inorg. Chem.* **1994**, *39*, 512–520.
- (24) O'Keeffe, M.; Eddaoudi, M.; Li, H.; Reineke, T. M.; Yaghi, O. M. Frameworks for Extended Solids: Geometrical design Principles. *J. Solid State Chem.* **2000**, *152*, 3–20.
- (25) O'Keeffe, M.; Hyde, B. G. *Crystal Structures. I. Patterns and symmetry*; Mineralogical Society of America: Washington, DC, 1996.
- (26) Li, H.; Davis, C. E.; Groy, T. L.; Kelley, D. G.; Yaghi, O. M. Coordinatively unsaturated metal centers in the extended porous framework of $\text{Zn}_3(\text{BDC})_3 \cdot 6\text{CH}_3\text{OH}$ (BDC = 1,4-benzenedicarboxylate). *J. Am. Chem. Soc.* **1998**, *120*, 2186–2187.
- (27) Eddaoudi, M.; Li, H.; Reineke, T.; Fehr, M.; Kelley, D.; Groy, T. L.; Yaghi, O. M. Design and synthesis of metal-carboxylate frameworks with permanent microporosity. *Top. Catal.* **1999**, *9*, 105–111.
- (28) Yaghi, O. M.; Davis, C. E.; Li, G.; Li, H. Selective guest binding by tailored channels in a 3-D porous zinc(II)-benzenetricarboxylate network. *J. Am. Chem. Soc.* **1997**, *119*, 2861–2868.
- (29) Eddaoudi, M.; Li, H.; Yaghi, O. M. Highly porous and stable metal-organic frameworks: structure design and sorption properties. *J. Am. Chem. Soc.* **2000**, *122*, 1391–1397.
- (30) Reineke, T. M.; Eddaoudi, M.; Fehr, M.; Kelley, D.; Yaghi, O. M. From condensed lanthanide coordination solids to microporous frameworks having accessible metal sites. *J. Am. Chem. Soc.* **1999**, *121*, 1651–1657.
- (31) Reineke, T. M.; Eddaoudi, M.; O'Keeffe, M.; Yaghi, O. M. A microporous lanthanide-organic framework. *Angew. Chem., Int. Ed.* **1999**, *38*, 2590–2594.
- (32) Li, H.; Eddaoudi, M.; Groy, T. L.; Yaghi, O. M. Establishing microporosity in open metal-organic frameworks: gas sorption isotherms for $\text{Zn}(\text{BDC})$ (BDC = 1,4-benzenedicarboxylate). *J. Am. Chem. Soc.* **1998**, *120*, 8571–8572.
- (33) Agterberg, F. P. W.; Provó Kluit, A. J.; Driessen, W. L.; Oevering, H.; Buijs, W.; Lakin, M. T.; Speck, A. L.; Reedijk, J. Dinuclear paddle-wheel copper(II) carboxylates in the catalytic oxidation of carboxylic acids. Unusual polymeric chains found in the single-crystal X-ray structures of [tetakis(μ -1-phenylcyclopropane-1-carboxylato-0,0')bis(ethanol-0)dycopper(II)] and catena-poly[[bis(μ -diphenylacetato-0,0')dycopper][μ_3 -diphenylacetato-1-0:2-0':1'-0')-(μ_3 -diphenylacetato-1-0:2-0':2'-0')]. *Inorg. Chem.* **1997**, *36*, 4321–4328.
- (34) Chen, B.; Eddaoudi, M.; Reineke, T. M.; Kampf, J. W.; O'Keeffe, M.; Yaghi, O. M. $\text{Cu}_2(\text{ATC}) \cdot 6\text{H}_2\text{O}$: Design of open metal sites in porous metal-organic crystals (ATC: 1,3,5,7-adamantane tetracarboxylate). *J. Am. Chem. Soc.* **2000**, *122*, 11559–11560.
- (35) Li, H.; Eddaoudi, M.; O'Keeffe, M.; Yaghi, O. M. Design and synthesis of an exceptionally stable and highly porous metal-organic framework. *Nature* **1999**, *402*, 276–279.
- (36) Harlow, R. L. Troublesome crystal structures: prevention, detection, and resolution. *J. Res. Natl. Inst. Stand. Technol.* **1996**, *101*, 327–339.

- (37) Reineke, T. M.; Eddaoudi, M.; Moler, D.; O'Keeffe, M.; Yaghi, O. M. Large free volume in maximally interpenetrating networks: the role of secondary building units exemplified by $\text{Tb}_2(\text{ADB})_3[(\text{CH}_3)_2\text{SO}]_4 \cdot 16[(\text{CH}_3)_2\text{SO}]$. *J. Am. Chem. Soc.* **2000**, *122*, 4843–4844.
- (38) Hyde, S. T.; Ninham, B.; Andersson, S.; Blum, Z.; Landh, T.; Larsson, K.; Lidin, S. *The Language of Shape*; Elsevier: Amsterdam. 1997.

AR000034B